Laboratory Investigation (2013) 93, 230–241

Spontaneous onset of nonalcoholic steatohepatitis and hepatocellular carcinoma in a mouse model of metabolic syndrome

Takeshi Nishida[1], Koichi Tsuneyama[1], Makoto Fujimoto[2], Kazuhiro Nomoto[1], Shinichi Hayashi[1], Shigeharu Miwa[1], Takahiko Nakajima[1], Yuko Nakanishi[1], Yoshiyuki Sasaki[3,4], Wataru Suzuki[3], Seiichi Iizuka[3], Mitsunobu Nagata[3], Tsutomu Shimada[3], Masaki Aburada[3], Yutaka Shimada[2] and Johji Imura[1]

Metabolic syndrome is a worldwide healthcare issue and a dominant risk factor for the development of incurable diseases that affect the entire body. The hepatic manifestations of this syndrome include nonalcoholic fatty liver disease (NAFLD) and its progressive variant nonalcoholic steatohepatitis (NASH). The basic pathogenesis of NAFLD/NASH remains controversial because it is difficult to clarify the disease process of NASH on the basis of metabolic syndrome alone. To determine the pathogenesis and effective treatment, an excellent animal model of NASH is required. Tsumura Suzuki obese diabetes (TSOD) male mice spontaneously develop diabetes mellitus, obesity, glucosuria, hyperglycemia, and hyperinsulinemia without any special treatments such as gene manipulation. In this study, we examined the histopathological characteristics of visceral fat and liver of 56 male TSOD mice aged 4–17 months and 9 male Tsumura Suzuki non-obesity (control) mice aged 6–12 months. In the visceral fat, enlargement of adipocytes and perivascular and pericapsular CD8-positive lymphoid aggregation were observed in 4-month-old mice. Abnormal expression of tumor necrosis factor-α, interleukin-6, and lipid peroxidation endo products was observed in macrophages. In the liver, microvesicular steatosis, hepatocellular ballooning, and Mallory bodies were observed in 4-month-old mice, with severity worsening with increasing time. These pathological findings in the liver mimic those seen in patients with NASH. Interestingly, small liver nodules with high cellularity and absence of portal tracts were frequently observed after 12 months. Most of them showed nuclear and structural atypia, and mimicked human hepatocellular carcinoma. The degree of steatosis in the non-tumor portions of the liver improved when the liver nodules developed. These findings were not observed in control mice. Here, we report that TSOD male mice spontaneously developed NAFLD without any special treatment, and that these mice are a valuable model for assessing NASH and NASH carcinogenesis owing to metabolic syndrome.

Laboratory Investigation (2013) **93,** 230–241; doi:10.1038/labinvest.2012.155; published online 19 November 2012

KEYWORDS: animal model; hepatocellular carcinoma; inflammation; nonalcoholic steatohepatitis; obesity; oxidative stress; type-2 diabetes

Metabolic syndrome starts with the accumulation of visceral fat and progresses to insulin resistance, hyperlipidemia, and various other disease conditions that affect the entire body. They depend mainly on quantitative changes in pro-inflammatory and anti-inflammatory adipocytokines secreted from enlarged adipocytes and infiltrating macrophages. The hepatic manifestations of metabolic syndrome include nonalcoholic fatty liver disease (NAFLD) and its progressive variant nonalcoholic steatohepatitis (NASH).[1,2] The pathogenesis of NASH is believed to involve a multistep process that begins with excessive accumulation of lipids in the liver. According to the two-hit theory,[3] the development

[1]Department of Diagnostic Pathology, Graduate School of Medicine and Pharmaceutical Sciences, University of Toyama, Toyama, Japan; [2]Department of Japanese Oriental Medicine, Graduate School of Medicine and Pharmaceutical Sciences, University of Toyama, Toyama, Japan; [3]Faculty of Pharmacy, Research Institute of Pharmaceutical Sciences, Musashino University, Tokyo, Japan and [4]Institute for Animal Reproduction, 1103 Fukaya, Kasumigaura-shi, Japan
Correspondence: Dr K Tsuneyama, MD, PhD, Department of Diagnostic Pathology, Graduate School of Medicine and Pharmaceutical Sciences, University of Toyama, 2630 Sugitani, Toyama 930 0194, Japan.
E-mail: ktsune@med.u-toyama.ac.jp

Received 10 May 2012; revised 21 September 2012; accepted 27 September 2012

of NASH requires the presence of additional pathogenic factors, such as oxidative stress, endotoxins, cytokines, and chemokines. Although significant research has been conducted, the basic pathogenesis of NAFLD/NASH remains controversial and effective treatments are still unavailable.

Pathologically, macro- and microvesicular steatoses are predominantly observed in zone 3 of the liver in NAFLD patients. In addition, hepatocellular ballooning degeneration, Mallory bodies, megamitochondria, lobular inflammation with neutrophils, and slender fibrous extensions of the perivenular and pericellular areas have been observed in patients with NASH.[4] Furthermore, patients with NASH are at a high risk of ultimately developing cirrhosis and hepatocellular carcinoma (HCC).[5,6] Although many studies have been conducted to investigate the mechanism of NASH, no firm conclusions have been reached yet because genetic and environmental factors involved in this disease are quite complicated.

To determine the pathogenesis and effective treatment, excellent animal models of NASH are required. Although several animal models have been proposed, many of them are based on genetic defects or special diet-induced factors, so it is difficult to determine the exact disease process of NASH on the basis of metabolic syndrome alone.[7–9] We previously described a murine model of NASH induced by neonatal subcutaneous injection of monosodium glutamate (MSG), which includes the clinical manifestations of central obesity, diabetes, hyperlipidemia, and ultimately, liver inflammation, fibrosis, and liver tumor, similar to the manifestations that are present in the human liver.[10,11]

Tsumura Suzuki obese diabetes (TSOD) mice are novel polygenic models of spontaneous type-2 diabetes mellitus that develop moderate degrees of obesity, especially apparent in animals more than 11 weeks of age.[12,13] Unlike MSG mice, male TSOD mice showed glycosuria, hyperglycemia, and hyperinsulinemia without any special treatments.[14] In addition, the pathological characteristics of these mice were also examined under severe circumstances because steatohepatitis and liver nodules were frequently observed in male TSOD mice during preliminary examination. In the present study, we conducted a detailed histopathological examination of the disease process in male TSOD mice. Here, we report that these mice are useful for studying the entire natural history of NASH and its carcinogenetic mechanism without any special treatment.

MATERIALS AND METHODS

Animals

Sixty-eight male TSOD mice and 15 male Tsumura Suzuki non-obesity (TSNO) mice were purchased from the Institute for Animal Reproduction (Ibaraki, Japan). TSOD mice were established in 1992 as an inbred strain from the *ddy* strain; TSNO mice were simultaneously established from the same strain as controls that show neither obesity nor hyperglycemia.[14] Two to three mice were housed in plastic cages in a non-barrier-sustained animal room that was maintained at $23 \pm 2\,^{\circ}C$ with $50 \pm 10\%$ relative humidity and a 12/12-h light/dark cycle. All mice were maintained on a basal diet MF (Oriental Yeast, Tokyo, Japan) and chlorinated water *ad libitum* before autopsy. This study was performed in accordance with the animal experiment guidelines specified by the University of Toyama. For histological analyses, TSOD mice were killed at 4 ($n=11$), 6 ($n=3$), 7 ($n=7$), 12 ($n=12$), 14 ($n=8$), 15 ($n=10$), 16 ($n=3$), and 17 ($n=2$) months of age and control TSNO mice were killed at 6 ($n=3$) and 12 ($n=6$) months of age. Additional TSOD and TSNO mice were killed at the age of 1 ($n=6$ and $n=3$) and 12 ($n=6$ and $n=3$) months for gene expression analysis. Body weights were recorded at the start and at the end of each experimental period. After killing, the liver and visceral fat were rapidly excised and rinsed in ice-cold saline. Body weights were measured only at 6 months of age. All excised organs were then fixed with 10% neutral-buffered formalin and embedded in paraffin for histological analysis. Selected liver samples were also made into frozen sections.

Histopathological and Immunohistochemical Analyses

The formalin-fixed, paraffin-embedded tissues were processed and 4-μm-thick serial sections were cut and stained with hematoxylin and eosin (HE) or Azan for fibrosis, while Sudan IV with hematoxylin counterstaining was used on frozen 5-μm-thick sections for lipid analysis. Liver histology was scored using the system proposed by the NASH Clinical Research Network[15] based on four semiquantitative items: steatosis (0–3), lobular inflammation (0–3), hepatocellular ballooning (0–2), and fibrosis (0–4). Three representative areas were scored in each section and the average values were used as the final score. The sum of the steatosis, lobular inflammation, and hepatocellular ballooning scores constituted the NAFLD activity score (NAS) (Table 1). A NAS value ≥ 5 was consistent with a diagnosis of NASH, while NAS <3 ruled out a diagnosis of NASH. The degree of liver fibrosis was evaluated using Azan staining. The following primary antibodies were used for immunohistochemical analysis: rat anti-mouse monoclonal antibodies for Mac2 as a marker of macrophages (1:100 dilution; Cedarlane, ON, Canada), CD8 (1:20 dilution; Acris Antibodies, Hiddenhausen), tumor necrosis factor (TNF)-α (1:50 dilution; Monosan, Uden, The Netherlands), interleukin (IL)-6 (1:20 dilution; R&D Systems, MN), rabbit polyclonal antibodies for glutamine synthetase (1:500 dilution; Millipore, CA), 4-hydroxy-2-nonenal (4-HNE as a marker of oxidative stress) (1:30 dilution; Nikken Seil, Japan), p62 as a marker of Mallory bodies (1:3000 dilution; Biomol International, PA), myeloperoxidase as a marker of neurtorophils (1:100 dilution; Dako, Denmark), Cytochrome P450 2E1 (CYP2E1) (1:100 dilution; Biomol International), and glutathione s-transferase pi (1:50 dilution; Novocastra, UK). Briefly, the sections were incubated with the primary antibodies in a wet

chamber for 60 min or more at room temperature. After rinsing with Tris-buffered saline containing 0.1% Tween (TBS-T), the sections were incubated with EnVision Peroxidase (PO) (for rabbit polyclonal antibodies) (Dako, Japan) or Histone simple stain MAX-PO (for rat monoclonal antibodies) (Nichirei, Japan) for 60 min or more at room temperature. After rinsing in TBS-T, 3,3′-diaminobenzidine (Sigma, Steinheim, Germany) was applied as a substrate for the PO.

RNA Preparation and Real-Time PCR

The mRNA expression of five genes related to inflammatory cytokines (TNF-α and IL-6) and transcription factors that participate in the development of hepatic steatosis (peroxisome proliferator-activated receptor alpha (PPARα), PPARγ, and sterol regulatory element-binding protein-1 (SREBP1)) were assessed by real-time PCR. Total RNA was isolated from the liver and visceral fat samples by using Isogen reagent (Nippon Gene, Japan). Complementary DNA was synthesized from 500 ng of total RNA by using a ReverTra Ace® qPCR RT Master Mix with gDNA Remover (Toyobo, Japan). PCR reactions and analyses were carried out using a LightCycler® Nano System (Roche, Japan) with denaturation for 10 min at 95 °C, followed by 45 PCR cycles of denaturation at 95 °C for 10 s, annealing at 60 °C for 10 s, and extension at 72 °C for 15 s. All primers used for analysis were designed at Sigma-Aldrich (Japan). The primer sequence details are presented in Supplementary Table 1.[16–18] The amount of mRNA was calculated using glyceraldehyde-3-phosphate dehydrogenese as an endogenous control.

Statistical Analyses

Values are expressed as mean ± s.e.m. Means were compared using the Mann–Whitney *U*-test. $P<0.05$ was considered statistically significant.

RESULTS

Histopathological Imaging of Visceral Fat

When compared with the visceral fat per body weight ratio at 6 months of age, TSOD mice had significantly greater ratios than TSNO mice of the same age (Table 2). In TSOD mice, visceral fat was remarkably enlarged compared with subcutaneous fat. Crown-like structures (CLSs), composed of Mac-2-positive macrophage aggregates, were also observed in some places in all 4-month-old mice (Figure 1a and Supplementary Figure 1). On the other hand, lipid droplets obtained from TSNO mice were smaller compared with those obtained from TSOD mice, and CLSs were occasionally observed at 6 months of age (Figure 1b). Moreover, perivascular and pericapsular lymphoid aggregations were occasionally observed in 4-month-old TSOD mice (Figure 1c). Immunohistochemically, these aggregated lymphocytes were mainly CD8-positive cells at 6 months of age (Figure 1d and Supplementary Figure 2). In addition, the macrophages that composed the CLSs expressed pro-inflammatory cytokines such as TNF-α (Figure 1e) and IL-6 (Figure 1f) in 6-month-

Table 1 NASH Clinical Research Network Scoring System

Item	*Definition*	*Score/code*
NAS		
Steatosis	Low- to medium-power evaluation of parenchymal involvement by steatosis	
	<5%	0
	5–33%	1
	>33–66%	2
	>66%	3
Lobular inflammation	Overall assessment of all inflammatory foci	
	No foci	0
	<2 foci per ×200 field	1
	2–4 foci per ×200 field	2
	>4 foci per ×200 field	3
Hepatocellular ballooning	None	0
	Few balloon cells	1
	Many cells/prominent ballooning	2
		Full score: 8
Fibrosis		
Stage	None	0
	Perisinusoidal or periportal	1
	Mild, zone 3, perisinusoidal	1A
	Moderate, zone 3, perisinusoidal	1B
	Portal/periportal	1C
	Perisinusoidal and portal/periportal	2
	Bridging fibrosis	3
	Cirrhosis	4

Abbreviations: NAS, NAFLD (nonalcoholic fatty liver disease) activity score; NASH, nonalcoholic steatohepatitis.

Table 2 Liver weight per body weight ratio and visceral fat weight per body weight ratio of TSOD and TSNO mice at 6 months of age

	TSNO	TSOD
Liver weight/body weight	40.520 ± 1.176	46.878 ± 3.843*
Visceral fat weight/body weight	14.225 ± 0.372	39.603 ± 3.104*

Results are expressed as mean ± s.e.m.
*$P<0.01$ in comparison with TSNO mice.

old TSOD mice. Lipid peroxidation endo products, such as 4-HNE, were expressed in several parts of enlarged adipocytes and aggregated macrophages in the visceral fat of TSOD mice (Figures 1g and h) at 6 months of age. TNF-α, IL-6, and 4-HNE were not expressed in the visceral fat of TSNO mice.

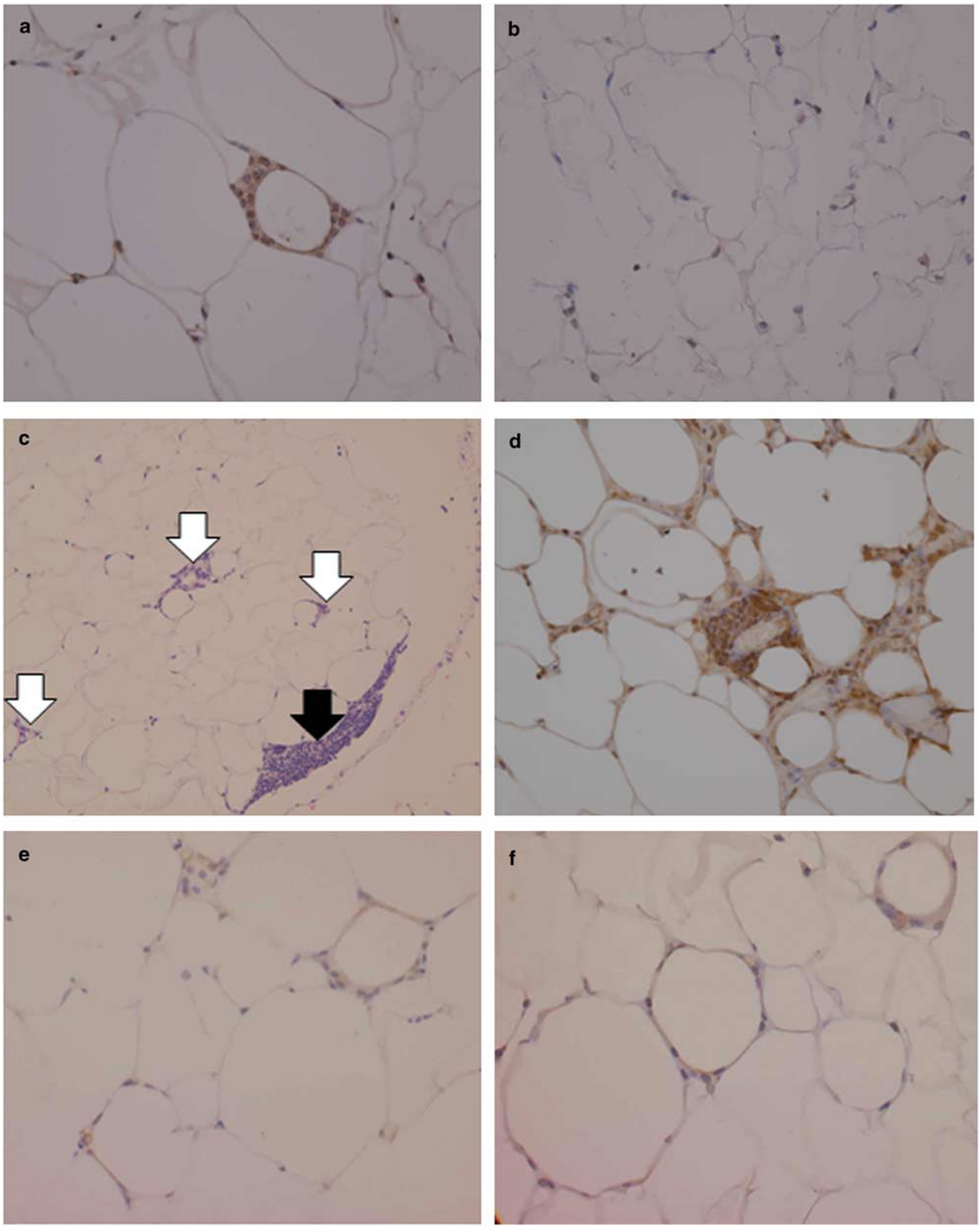

Figure 1 For caption please refer page 234.

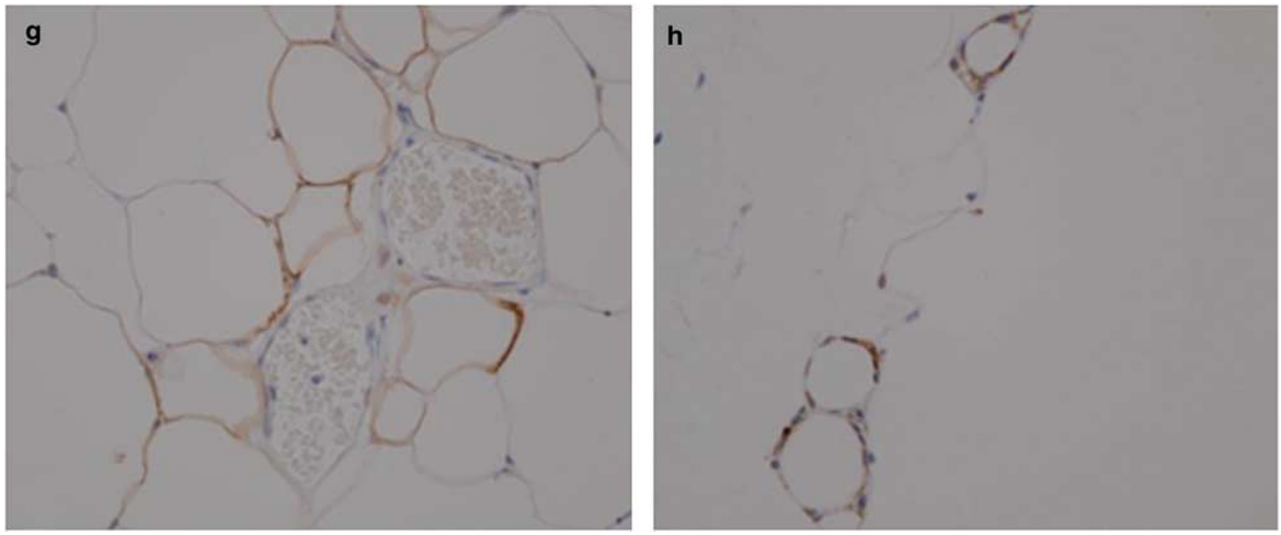

Figure 1 Micrographs of visceral fat of TSOD mice and TSNO mice at 4 (**a**, **c**) and 6 (**b**, **d**, **e**–**h**) months of age. (**a**) Adipocytes are remarkably enlarged and Mac-2-positive macrophages aggregated to form crown-like structures are observed in TSOD mice (× 400 magnification; Mac-2 immunostaining). (**b**) Each adipocyte is small, and crown-like structures are occasionally observed in TSNO mice (× 400 magnification; Mac-2 immunostaining). (**c**) Lymphoid aggregates in perivascular (white arrows) and pericapsular (black arrow) areas of TSOD mice (× 200 magnification; HE staining). (**d**) Aggregated lymphocytes in TSOD mice are mainly CD8-positive (× 400 magnification; CD8 immunostaining). TNF-α (**e**) and IL-6 (**f**) are expressed in the aggregated macrophages of TSOD mice (× 400 magnification; TNF-α and IL-6 immunostaining). Lipid peroxidation endo products, such as 4-HNE, are expressed in several parts of enlarged adipocytes (**g**) and aggregated macrophages (**h**) in the visceral fat of TSOD mice (× 400 magnification; 4-HNE immunostaining).

Histopathological Imaging of the Liver

The liver weight per body weight ratio in TSOD mice at 6 months of age was significantly greater compared with that in TSNO mice (Table 2). In TSOD mice, microvesicular fatty changes were recognized in the hepatocytes in zone 3 of 4-month-old mice. Scattered hepatocellular ballooning degeneration and Mallory bodies were also observed. At around 6 months of age, macro- and microvesicular steatosis (Figures 2a and b), hepatocellular ballooning degeneration (Figure 2c), and Mallory bodies (Figure 2d and Supplementary Figure 3) were worse than those observed in 4-month-old mice. In addition, neutrophil aggregation and necroinflammatory changes were observed sporadically in 6-month-old mice (Figures 2e and f). In 12-month-old mice, micro- and macrovesicular steatoses were frequently observed in the liver (Figure 2g). Although steatosis was observed in 14-month-old mice, its appearance ratio subsequently decreased. Necroinflammation and ballooning degeneration were observed to various degrees. Moreover, slight fibrosis was also observed after 12 months of age although there was individual specificity (data not shown). Interestingly, well-demarcated, whitish-yellow liver nodules were frequently observed (Figure 3a). These nodules were composed of trabecular arrangements of atypical hepatocytes without portal tractsinside (Figures 3b and c). They were diagnosed as dysplastic nodules. After 12 months of age, the frequency of the liver nodules increased with time. Most liver nodules in mice over 16 months of age were yellow or green and irregularly shaped (Figures 3d and e). Pathologically, these nodules were composed of atypical hepatocytes with higher cellularity and structural atypia in a thick trabecular or pseudoglandular pattern (Figures 3f and g). Moreover, glutamine synthetase and GST-pi, which are one of the useful markers of differential diagnosis for HCC,[19,20] were expressed in these areas (Figure 4 and Supplementary Figure 4). These liver nodules shared a number of pathological characteristics with human HCC. Interestingly, the degree of steatosis in the non-tumor portions of the liver improved when the liver nodules developed (Figure 5). On the other hand, these characteristics, including steatosis, ballooning degeneration, fibrosis, and liver nodules, were not observed in TSNO mice.

Evaluation of NAS Score

In TSOD mice, although the prevalence of an NAS score ≥ 3 gradually increased till 12 months of age, this rate decreased in TSOD mice older than 14 months. Some 12-month-old TSOD mice showed a NAS score of ≥ 5. On the other hand, both 6-month-old and 12-month-old TSNO mice had NAS scores ≤ 1. There was no definitive evidence of NAFLD in the TSNO mice (Table 3).

Validation of Gene Expression with Real-Time PCR

Visceral fat mRNA levels for TNF-α and IL-6 were significantly increased in TSOD mice compared with TSNO mice at 12 months of age (Figures 6a and b). These data

suggest that an overexpression of TNF-α and IL-6 was induced in enlarged adipocytes. Hepatic mRNA levels for PPARγ were significantly increased in TSOD mice compared with TSNO mice at 12 months of age (Figure 6c). Hepatic mRNA levels for PPARα and SREBP1 were also elevated in TSOD mice at 12 months of age compared with TSNO mice (Figures 6d and e), although significant differences were not observed.

DISCUSSION

NAFLD and its progressive state, NASH, are believed to be the phenotypes of metabolic syndrome in the liver, and the number of patients affected by these two conditions is constantly increasing. In Japan, 10–30% of the population with metabolic syndrome is believed to have NAFLD accompanying metabolic syndrome, and 10% of this population is presumed to have NASH.[21] Although there are many unclear points regarding the pathogenic mechanism of NASH, the two-hit theory, according to which fat first accumulates in hepatocytes as a consequence of overeating, hyperlipidemia, and other factors, and then the pathological condition progresses because of the second hit, such as oxidative stress, is widely accepted.[3] As effective treatments for NASH have not yet been established, dietary counseling and therapeutic

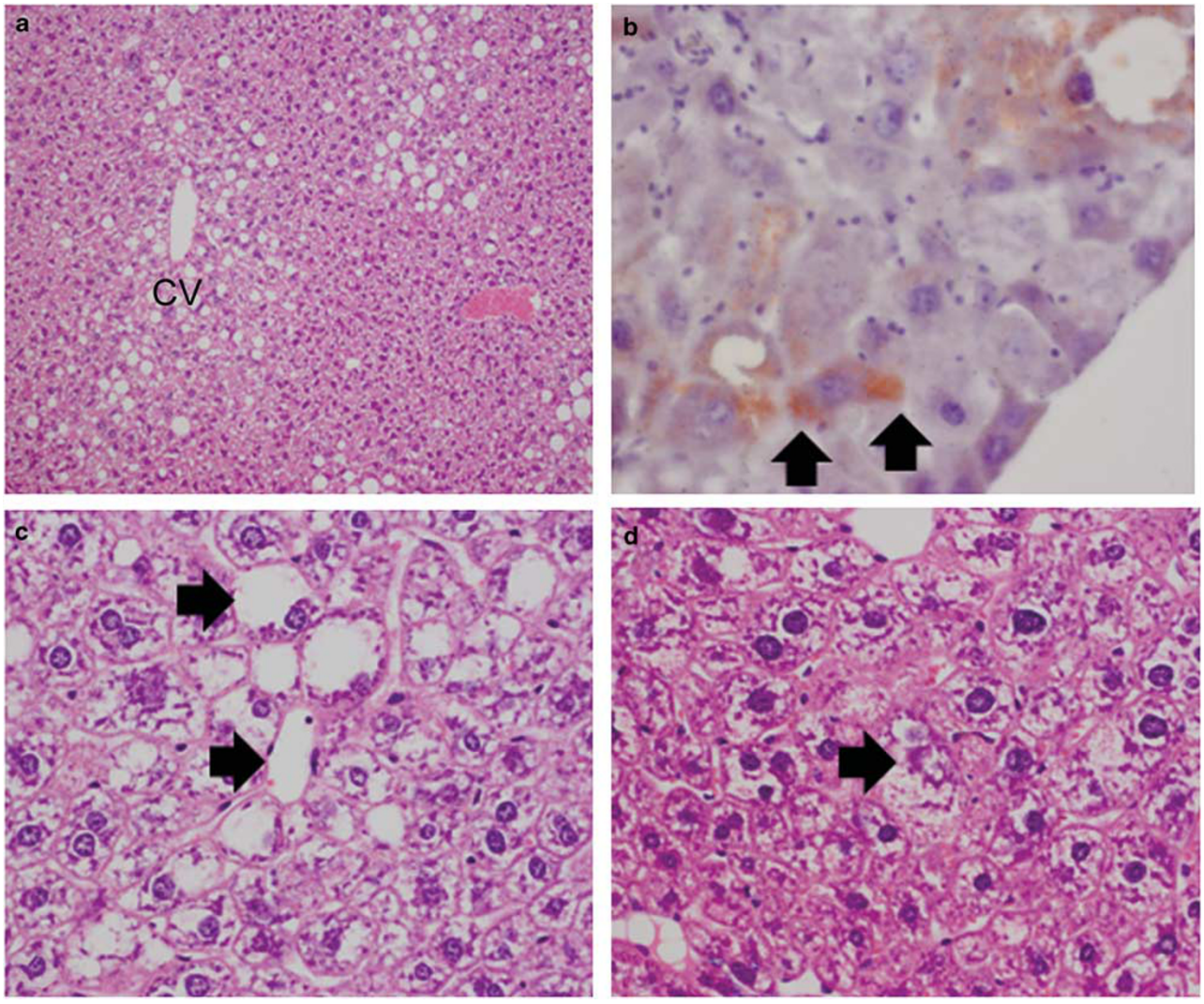

Figure 2 Micrographs of the livers of TSOD mice. (**a**) Macro- and microvesicular fatty changes were observed in hepatocytes in zone 3 at 6 months of age (×100 magnification; HE staining; CV, central vein). (**b**) Sudan IV-stained frozen section showing micro lipid droplets (black arrows) within hepatocytes in the perivenular area at 6 months of age (×400 magnification; Sudan IV staining). (**c**) Ballooning degeneration (black arrows) were observed at 6 months of age (×400 magnification; HE staining). (**d**) Mallory bodies (black arrow) were observed at 6 months of age (×400 magnification; HE staining). (**e**) Neutrophil aggregation is sporadically observed (×400 magnification; myeloperoxidase immunostaining for neutrophil markers). (**f**) Necroinflammatory changes, such as apoptotic bodies (black arrow), are sporadically observed (×400 magnification; HE staining). (**g**) In 12-month-old mice, micro- to macrovesicular steatosis is frequently observed in the liver. Necroinflammation and ballooning degeneration were observed to various degrees (×400 magnification; HE staining).

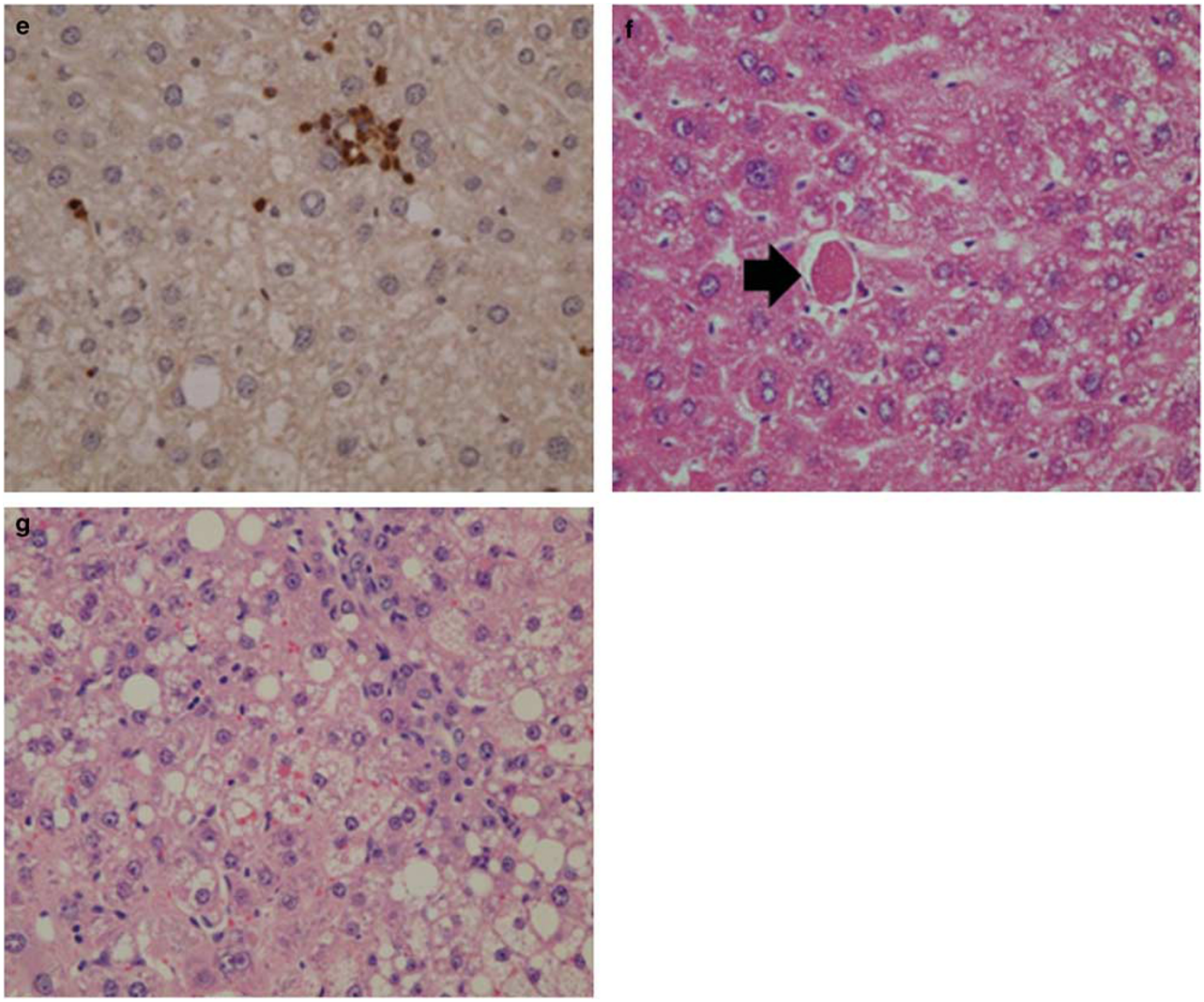

Figure 2 (Continued)

exercise are usually considered as the first options.[22–24] However, adhering to a continuous and strict therapy based on lifestyle improvements is difficult, and the response rate is not always high. In the case of NASH with a background of metabolic syndrome, administration of medications that treat underlying diseases, such as diabetes and obesity, has also been attempted. However, in large-scale clinical trials of pioglitazone, the effects remain uncertain because, for example, simultaneous weight gain with improvement of liver damage has been reported.[25–27] An excellent animal model is urgently required to investigate the disease mechanism and determine prompt remedies.

Various kinds of animal models have been proposed; however, most of them are quite artificial owing to inheritable genetic modifications or the necessity of a special diet that lacks several essential amino acids.[7] In addition, almost all of these models did not develop obesity or metabolic syndrome similar to humans. We recently proposed an MSG-induced mouse model of NASH based on obesity, type-2 diabetes, and hyperlipidemia. In brief, neonatal subcutaneous injection of MSG induces obesity, type-2 diabetes, and hyperlipidemia in mice till 3–4 months of age without any other special treatment. All male MSG mice showed marked steatosis, lobular inflammation, Mallory bodies, and hepatocellular ballooning in 4–6 months of age, which are identical to the pathological findings observed in humans with NASH. In addition, dysplastic nodules were frequently observed around 12 months of age. MSG mice were excellent NASH animal models and showed a disease process similar to that observed in human NASH patients.[11] However, the disease mechanism with regard to why neonatal MSG injection induces metabolic syndrome is still unclear.

TSOD mice were established as an inbred line in 1992 by Suzuki *et al.*[14] in Japan and some of their clinical diabetic characteristics have been described. Only male TSOD mice

showed spontaneous obesity, glucosuria, hyperglycemia, and hyperinsulinemia.[14] Miura *et al.*[12] reported that the insulin-stimulated translocation of glucose transporter (GLUT)-4 from low-density microsomal membranes to plasma membranes was reduced in both the skeletal muscle and adipose tissue of TSOD mice and that the reduced insulin sensitivity was presumably owing to this impaired GLUT-4 translocation in both the skeletal muscle and adipocytes. Using a genome-wide screen for loci linked to glucose homeostasis and body weight in TSOD mice, Hirayama *et al.*[28] mapped three quantitative trait loci involved in diabetes mellitus. The major genetic determinants of blood glucose levels, insulin levels, and body weight were identified on chromosome 11, chromosome 2, and chromosome 1 and 2, respectively. In addition, Iizuka *et al.*[29] reported that TSOD mice showed spontaneous non-insulin-dependent diabetes mellitus with severe motor neuropathy and hypertrophy of pancreatic islets owing to proliferation and swelling of β cells. On the other hand, morphological evidence found in the livers of male TSOD mice has not yet been investigated in detail. In the present study, we attempted to clarify the morphological characteristics of the liver and visceral fat in male TSOD mice.

Interestingly, male TSOD mice developed not only remarkable obesity and diabetic symptoms but also steatohepatitis, including zone 3 microvesicular fatty changes, hepatocellular ballooning degeneration, Mallory bodies, and inflammatory cell infiltration such as neutrophil aggregation after 4 months of age. These findings suggest that the livers of TSOD mice have histopathological characteristics similar to

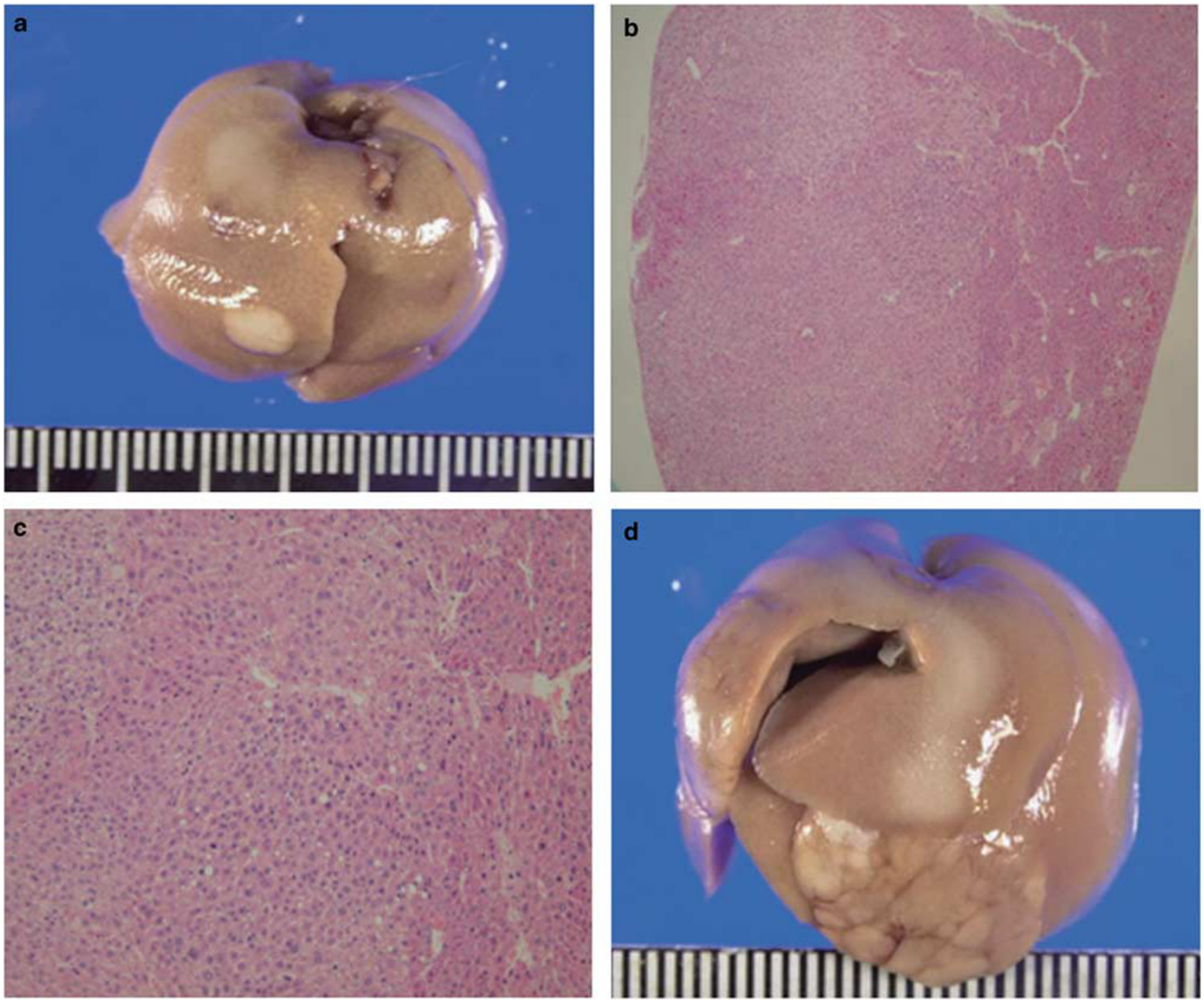

Figure 3 Macroscopic appearance (**a**, **d**, **e**) and histology (**b**, **c**, **f**, **g**) of liver nodules in TSOD mice. (**a**) Whitish-yellow well-demarcated liver nodules are frequently observed. (**b**, **c**) Micrographs of liver nodules. These are composed of trabecular arrangement of atypical hepatocytes with no portal tracts inside (**b** $\times$40 magnification, **c** $\times$200 magnification; HE staining). Liver tumor showing yellow color (**d**) or green color (**e**) nodules with an irregular shape is observed in 16-month-old mice. Histopathologically, these nodules are composed of atypical hepatocytes with higher cellularity and structural atypia showing a thick trabecular or pseudoglandular pattern (**f**, **g**).

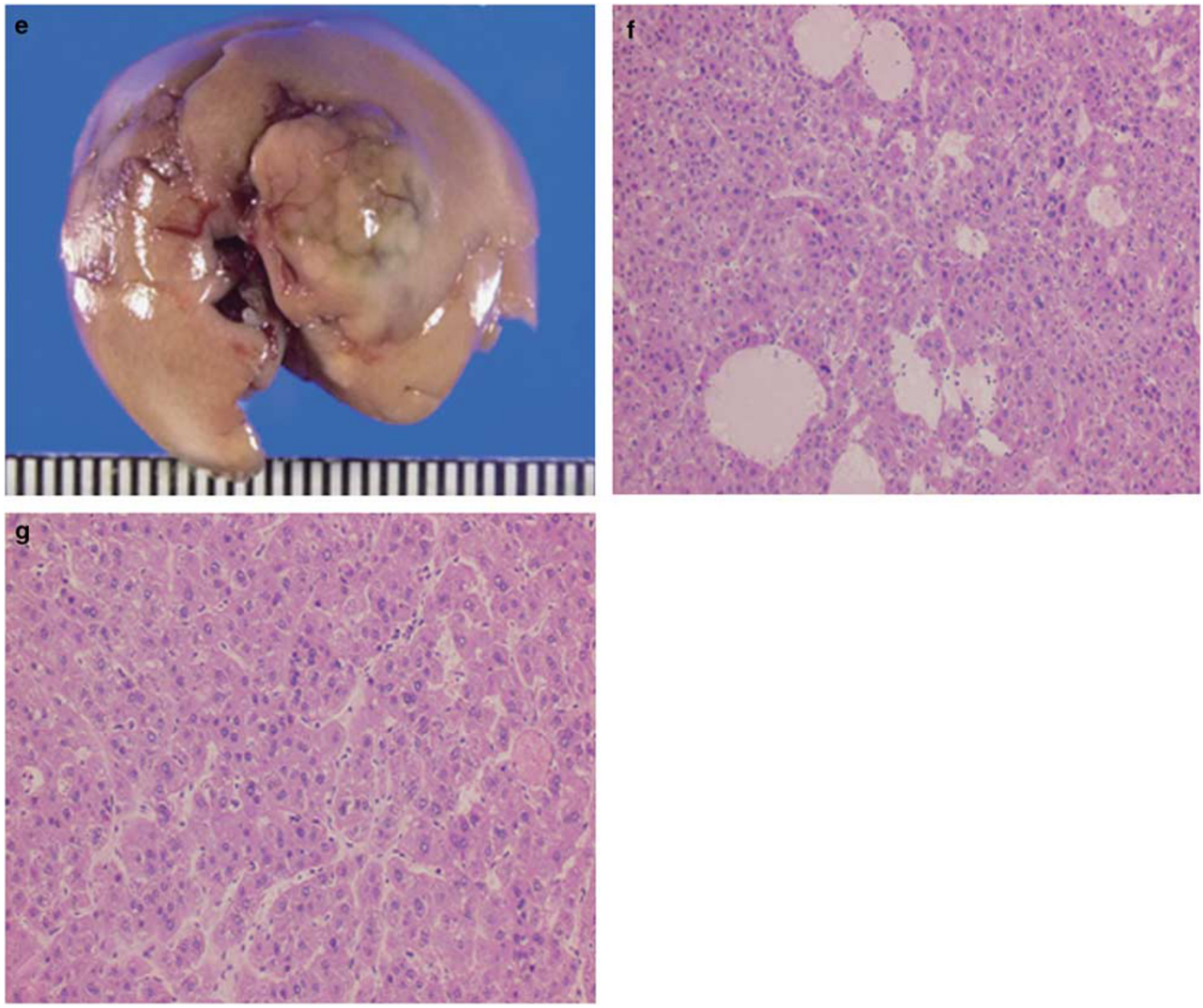

Figure 3 (Continued)

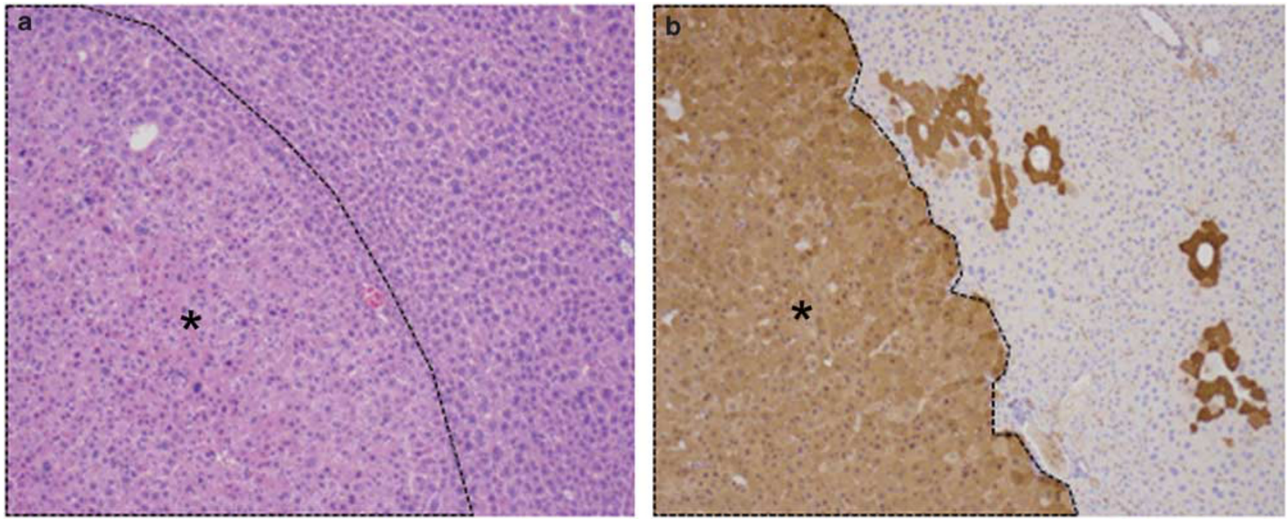

Figure 4 Comparison of the same liver nodule area in TSOD mice by both HE staining (**a**) and glutamine synthetase staining (**b**). Glutamine synthetase was expressed in accordance with the liver nodules area (asterisk) (**a**, **b** × 100 magnification).

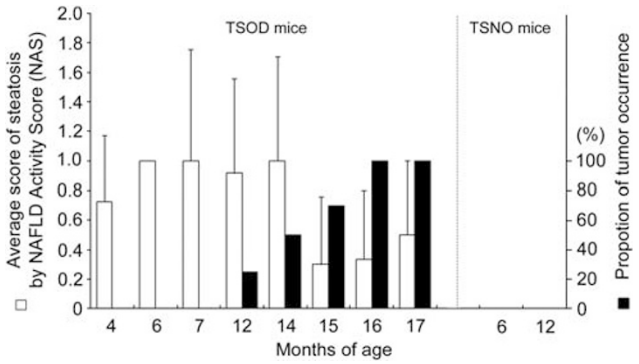

Figure 5 Time course of average score of steatosis estimated by NAFLD activity score (white columns) and proportion of tumor appearance (black columns) in TSOD and TSNO mice. Steatosis in the liver has been improved when the age of TSOD mice were passed over 12 months. On the other hand, the liver nodules frequently appeared after 12 months of age in TSOD mice.

those found in humans with NASH, although liver fibrosis was weakly present in histopathological evaluations in old TSOD mice.

It has been reported that PPARγ is an important determinant of hepatic fat accumulation and that hepatic PPARγ expression is increased in experimental models of fatty liver disease.[30–32] In the present study, 12-month-old TSOD mice exhibited increased hepatic mRNA levels for PPARγ compared with TSNO mice of the same age. Furthermore, the hepatic staining intensity by CYP2E1 immunostaining is slightly greater in TSOD mice than in TSNO mice at both 6 and 12 months of age (Supplementary Figure 5). Thus far, it has been reported that blood TG levels in TSOD mice are greater than those in TSNO mice.[29,33] These data suggest that the hepatic dysfunction observed early in time is associated with the development of fatty liver disease in TSOD mice. In the visceral fat, enlargement of adipocytes, perivascular and pericapsular CD8-positive lymphoid aggregations, and CLSs with macrophage aggregation were observed after 4 months of age. Recently, Nishimura *et al.*[34] reported that CD8-positive lymphocytes contributed to macrophage recruitment and adipose tissue inflammation. Our results also showed that CD8-positive cells were associated with recruitment of macrophages and that adipose tissue with the macrophage aggregations was in a continuous state of inflammation owing to be secreted various pro-inflammatory cytokines. In fact, expression of inflammatory cytokines, such as TNF-α and IL-6, also increased with increasing mRNA levels. Moreover, the macrophages that compose the CLSs had aberrantly expressed 4-HNE, which indicates local oxidative stress. As blood from visceral fat runs through the liver via the portal vein, oxidative stress-induced cytokines produced in other tissues may accumulate in the liver. Following lipid accumulation in the livers of male TSOD mice, additional second hits, such as oxidative stress, may cause the liver pathology to develop into NASH, similar to that observed in humans.

Table 3 Score assessment of steatosis, lobular inflammation, hepatocellular ballooning, and NAS in TSOD mice and TSNO mice.

Score	Steatosis (0–3)		Lobular inflammation (0–3)		Hepatocellular ballooning (0–2)		NAS		
	(0–1)	(2–3)	(0–1)	(2–3)	0	(1–2)	≦1	2	3≦
TSOD mice (4 months; n = *11)*									
N	11	0	11	0	3	8	2	4	5
(%)	100	0	100	0	27.3	72.7	18.2	36.4	45.4
TSOD mice (6 months; n = *3)*									
N	3	0	3	0	0	3	0	1	2
(%)	100	0	100	0	0	100	0	33.3	66.7
TSOD mice (7 months; n = *7)*									
N	5	2	7	0	2	5	2	0	5
(%)	71.4	28.6	100	0	28.6	71.4	28.6	0	71.4
TSOD mice (12 months; n = *12)*									
N	10	2	12	0	2	10	2	1	9
(%)	83.3	16.7	100	0	16.7	83.3	16.7	8.3	75
TSOD mice (14 months; n = *8)*									
N	6	2	8	0	2	6	2	0	6
(%)	75	25	100	0	25	75	25	0	75
TSOD mice (15 months; n = *10)*									
N	10	0	10	0	2	8	2	5	3
(%)	100	0	100	0	20	80	20	50	30
TSOD mice (16 months; n = *3)*									
N	3	0	3	0	1	2	1	1	1
(%)	100	0	100	0	33.3	66.7	33.3	33.3	33.3
TSOD mice (17 months; n = *2)*									
N	2	0	2	0	0	2	0	1	1
(%)	100	0	100	0	0	100	0	50	50
TSNO mice (6 months; n = *3)*									
N	3	0	3	0	3	0	3	0	0
(%)	100	0	100	0	100	0	100	0	0
TSNO mice (12 months; n = *6)*									
N	6	0	6	0	6	0	6	0	0
(%)	100	0	100	0	100	0	100	0	0

Abbreviations: NAS, NAFLD (nonalcoholic fatty liver disease) activity score; TSNO, Tsumura Suzuki no obesity; TSOD, Tsumura Suzuki obese diabetes.

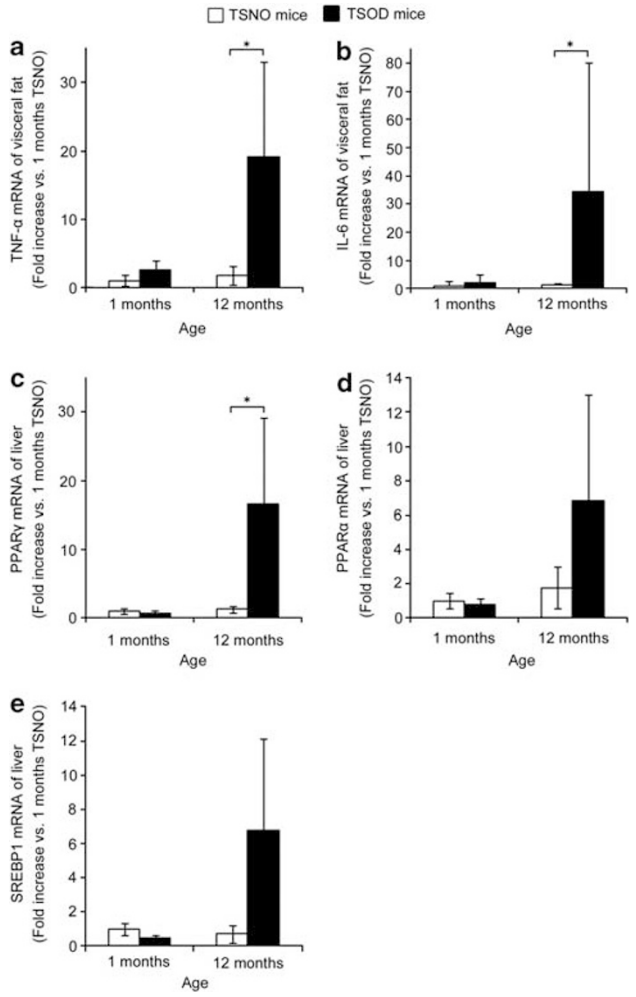

Figure 6 TNF-α (**a**) and IL-6 (**b**) mRNA levels in visceral fat and PPARγ (**c**), PPARα (**d**), and SREBP1 (**e**) mRNA levels in liver. The mRNA levels were determined by real-time PCR, normalized to glyceraldehyde-3-phosphate dehydrogenase, and expressed as folds of induction relative to that in TSNO mice at 1 month of age (3–6 mice in each group). *Significantly different from TSNO mice of the same age with a $P<0.05$. PPAR, peroxisome proliferator-activated receptor; SREBP, sterol regulatory element-binding protein.

TSOD mice developed liver tumors following steatohepatitis after 12 months of age. Demarcated nodules that were whitish-yellow or greenish in color were composed of atypical hepatocytes. Most of these nodules showed similar pathological findings to dysplastic nodules found in humans. Several liver nodules in 14-month-old mice demonstrated a thick trabecular or pseudoglandular pattern with various kinds of nuclear atypia. Glutamine synthetase, overexpressed in these liver nodules area, has been reported as a target of β-catenin signaling, which is implicated in the development of HCC.[35,36] Hepatocellular adenoma (HCA), including β-catenin-activated HCA subtype, is known as a benign liver neoplasm; however, this HCA subtype has an increased risk of malignant transformation, compared with the other subtypes.[37] Thus, we should possibly take into consideration that the liver nodules of TSOD mice are developed from β-catenin-activated HCA to HCC. In any case, these pathological findings were similar to human patients, taken together, the liver nodules of TSOD male mice may exhibit dysplastic nodule-carcinoma sequences. Interestingly, the degree of steatosis improved inversely as liver nodules developed. Similar findings were also observed in male MSG mice and galectin-3-knockout mice.[11,38,39] The characteristic histological features of steatohepatitis, such as steatosis or necroinflammatory changes, were often totally absent in the end stage in NASH patients. This phenomenon is known as 'burn-out NASH'.[40–42] TSOD mice may share the same mechanism as burn-out NASH.

In conclusion, TSOD male mice spontaneously developed NASH and HCC owing to obesity, type-2 diabetes, and hyperlipidemia. Neither gene alteration nor a special diet was required in this model, so we conclude that male TSOD mice are a valuable model for examining disease mechanisms and drug effectiveness.

Supplementary Information accompanies the paper on the Laboratory Investigation website (http://www.laboratoryinvestigation.org)

ACKNOWLEDGEMENTS

We thank Tokimasa Kumada, Hideki Hatta, and Chieko Kiya for their help and technical assistance in the experiments. We would also like to thank Yukari Inoue for her support during the preparation of this manuscript. We would like to express our appreciation to Dr Ulrich Deuschle (Phenex Pharmaceuticals AG, Germany) for his valuable advice. The project was supported in part by Grant-in Aid-for Scientific Research (B and C), Japan Society for the Promotion Science (24390181 and 21590433), Takeda Science Foundation, Japan (2010), and TSOD Mouse Research Fund.

DISCLOSURE/CONFLICT OF INTEREST

The authors declare no conflict of interest.

1. Ong JP, Younossi ZM. Epidemiology and natural history of NAFLD and NASH. Clin Liver Dis 2007;11:1–16, vii.
2. Charlton M. Nonalcoholic fatty liver disease: a review of current understanding and future impact. Clin Gastroenterol Hepatol 2004;2:1048–1058.
3. Day CP, James OF. Steatohepatitis: a tale of two 'hits'? Gastroenterology 1998;114:842–845.
4. Brunt EM. Nonalcoholic steatohepatitis: definition and pathology. Semin Liver Dis 2001;21:3–16.
5. Farrell GC, Larter CZ. Nonalcoholic fatty liver disease: from steatosis to cirrhosis. Hepatology 2006;43:S99–S112.
6. Bugianesi E. Non-alcoholic steatohepatitis and cancer. Clin Liver Dis 2007;11:191–207, x–xi.
7. Anstee QM, Goldin RD. Mouse models in non-alcoholic fatty liver disease and steatohepatitis research. Int J Exp Pathol 2006;87:1–16.
8. Deng QG, She H, Cheng JH, *et al.* Steatohepatitis induced by intragastric overfeeding in mice. Hepatology 2005;42:905–914.
9. Itoh M, Suganami T, Nakagawa N, *et al.* Melanocortin 4 receptor-deficient mice as a novel mouse model of nonalcoholic steatohepatitis. Am J Pathol 2011;179:2454–2463.
10. Nagata M, Suzuki W, Iizuka S, *et al.* Type 2 diabetes mellitus in obese mouse model induced by monosodium glutamate. Exp Anim 2006; 55:109–115.
11. Nakanishi Y, Tsuneyama K, Fujimoto M, *et al.* Monosodium glutamate (MSG): a villain and promoter of liver inflammation and dysplasia. J Autoimmun 2008;30:42–50.

12. Miura T, Suzuki W, Ishihara E, *et al.* Impairment of insulin-stimulated GLUT4 translocation in skeletal muscle and adipose tissue in the Tsumura Suzuki obese diabetic mouse: a new genetic animal model of type 2 diabetes. Eur J Endocrinol 2001;145:785–790.
13. Takahashi A, Tabuchi M, Suzuki W, *et al.* Insulin resistance and low sympathetic nerve activity in the Tsumura Suzuki obese diabetic mouse: a new model of spontaneous type 2 diabetes mellitus and obesity. Metabolism 2006;55:1664–1669.
14. Suzuki W, Iizuka S, Tabuchi M, *et al.* A new mouse model of spontaneous diabetes derived from ddY strain. Exp Anim 1999;48: 181–189.
15. Kleiner DE, Brunt EM, Van Natta M, *et al.* Design and validation of a histological scoring system for nonalcoholic fatty liver disease. Hepatology 2005;41:1313–1321.
16. Ramadori P, Ahmad G, Ramadori G. Cellular and molecular mechanisms regulating the hepatic erythropoietin expression during acute-phase response: a role for IL-6. Lab Invest 2010;90:1306–1324.
17. Shimada T, Tokuhara D, Tsubata M, *et al.* Flavangenol (pine bark extract) and its major component procyanidin B1 enhance fatty acid oxidation in fat-loaded models. Eur J Pharmacol 2012;677:147–153.
18. Yang ZH, Miyahara H, Hatanaka A. Chronic administration of palmitoleic acid reduces insulin resistance and hepatic lipid accumulation in KK-Ay mice with genetic type 2 diabetes. Lipids Health Dis 2011;10:120.
19. Di Tommaso L, Franchi G, Park YN, *et al.* Diagnostic value of HSP70, glypican 3, and glutamine synthetase in hepatocellular nodules in cirrhosis. Hepatology 2007;45:725–734.
20. Tremosini S, Forner A, Boix L, *et al.* Prospective validation of an immunohistochemical panel (glypican 3, heat shock protein 70 and glutamine synthetase) in liver biopsies for diagnosis of very early hepatocellular carcinoma. Gut 2012;61:1481–1487.
21. Sugimoto K, Takei Y. Clinicopathological features of non-alcoholic fatty liver disease. Hepatol Res 2011;41:911–920.
22. Yoneda M, Fujita K, Iwasaki T, *et al.* Treatment of NASH: nutritional counseling and physical exercise. Nihon Rinsho 2006;64:1139–1145.
23. Centis E, Marzocchi R, Di Domizio S, *et al.* The effect of lifestyle changes in non-alcoholic fatty liver disease. Dig Dis 2010;28:267–273.
24. Dowman JK, Armstrong MJ, Tomlinson JW, *et al.* Current therapeutic strategies in non-alcoholic fatty liver disease. Diabetes Obes Metab 2011;13:692–702.
25. Yki-Jarvinen H. Thiazolidinediones and the liver in humans. Curr Opin Lipidol 2009;20:477–483.
26. Sanyal AJ, Chalasani N, Kowdley KV, *et al.* Pioglitazone, vitamin E, or placebo for nonalcoholic steatohepatitis. N Engl J Med 2010;362: 1675–1685.
27. Shah P, Mudaliar S. Pioglitazone: side effect and safety profile. Expert Opin Drug Saf 2010;9:347–354.
28. Hirayama I, Yi Z, Izumi S, *et al.* Genetic analysis of obese diabetes in the TSOD mouse. Diabetes 1999;48:1183–1191.
29. Iizuka S, Suzuki W, Tabuchi M, *et al.* Diabetic complications in a new animal model (TSOD mouse) of spontaneous NIDDM with obesity Exp Anim 2005;54:71–83.
30. Gazit V, Huang J, Weymann A, *et al.* Analysis of the role of hepatic PPARgamma expression during mouse liver regeneration. Hepatology 2012;56:1489–1498.
31. Memon RA, Tecott LH, Nonogaki K, *et al.* Up-regulation of peroxisome proliferator-activated receptors (PPAR-alpha) and PPAR-gamma messenger ribonucleic acid expression in the liver in murine obesity: troglitazone induces expression of PPAR-gamma-responsive adipose tissue-specific genes in the liver of obese diabetic mice. Endocrinology 2000;141:4021–4031.
32. Inoue M, Ohtake T, Motomura W, *et al.* Increased expression of PPARgamma in high fat diet-induced liver steatosis in mice. Biochem Biophys Res Commun 2005;336:215–222.
33. Shimada T, Kudo T, Akase T, *et al.* Preventive effects of Bofutsushosan on obesity and various metabolic disorders. Biol Pharm Bull 2008;31:1362–1367.
34. Nishimura S, Manabe I, Nagasaki M, *et al.* CD8+ effector T cells contribute to macrophage recruitment and adipose tissue inflammation in obesity. Nat Med 2009;15:914–920.
35. Cadoret A, Ovejero C, Terris B, *et al.* New targets of beta-catenin signaling in the liver are involved in the glutamine metabolism. Oncogene 2002;21:8293–8301.
36. Zucman-Rossi J, Benhamouche S, Godard C, *et al.* Differential effects of inactivated Axin1 and activated beta-catenin mutations in human hepatocellular carcinomas. Oncogene 2007;26:774–780.
37. Zucman-Rossi J, Jeannot E, Nhieu JT, *et al.* Genotype-phenotype correlation in hepatocellular adenoma: new classification and relationship with HCC. Hepatology 2006;43:515–524.
38. Nomoto K, Tsuneyama K, Abdel Aziz HO, *et al.* Disrupted galectin-3 causes non-alcoholic fatty liver disease in male mice. J Pathol 2006; 210:469–477.
39. Nakanishi Y, Tsuneyama K, Nomoto K, *et al.* Nonalcoholic steatohepatitis and hepatocellular carcinoma in galectin-3 knockout mice. Hepatol Res 2008;38:1241–1251.
40. Abdelmalek M, Ludwig J, Lindor KD. Two cases from the spectrum of nonalcoholic steatohepatitis. J Clin Gastroenterol 1995;20: 127–130.
41. Yoshioka Y, Hashimoto E, Yatsuji S, *et al.* Nonalcoholic steatohepatitis: cirrhosis, hepatocellular carcinoma, and burnt-out NASH. J Gastroenterol 2004;39:1215–1218.
42. Powell EE, Cooksley WG, Hanson R, *et al.* The natural history of nonalcoholic steatohepatitis: a follow-up study of forty-two patients for up to 21 years. Hepatology 1990;11:74–80.